Engineering and Technology Journal e-ISSN: 2456-3358
Volume 06 Issue 06 June-2021, Page No.-925-931
DOI: 10.47191/etj/v6i6.06, I.F. – 6.39

Synthesis of Functional Nanoparticles for Application in Inkjet Printing

Chinh Dung Trinh[1,2,*], Dung My Thi Dang[1], Chien Mau Dang[1]

[1]Institute for Nanotechnology, Vietnam National University - Ho Chi Minh City, Community 6, Linh Trung Ward, Thu Duc District, Ho Chi Minh City, Vietnam

[2]University of Science, Vietnam National University - Ho Chi Minh City, 227 Nguyen Van Cu Street, Ward 4, District 5, Ho Chi Minh City, Vietnam

ABSTRACT: Ag nanoflakes were synthesized by chemical reduction method using cetyltrimethylammonium bromide (CTAB) as a surfactant. The results of transmission electron microscope (TEM) analysis, ultraviolet-visible spectroscopic (UV-Vis) analysis, X-ray diffraction (XRD) analysis showed that the obtained Ag nanoflakes had size of ~50 – 60 nm, thickness of 16 nm, with flake shape reached 96 %. The particles crystallized in cubic structure of Ag. The Ag nanoflakes synthesized with pH = 4 were dispersed stably after 60 days from synthesis. The properties of the obtained Ag nanoflakes were suitable for using them as conductive particles in fabrication of functional inks for electrohydrodynamic printing technique.

KEYWORDS: Nano flakes, Silver ink, Inkjet printing.

1. INTRODUCTION

Ink-jet printing technology has a long development history with many advantages, allowing high quality printing on various materials such as paper and textile. In the recent years, scientists have been interested in applying this technique in various high technologies such as electronics, biology, and nanotechnology [1-8]. These new applications have just been developed in the recent years based on the idea of using printers that can control ink droplets with volume of several picoliter containing desired materials to drop at exact positions on substrate following a template. The inks contain functional materials with desired structure and electrical, optical, chemical, and biological properties. This process uses a computer to control the jetting of inks, allowing easy printing of complicated templates. The technique shows a potential to print metal electronic boards that open up various applications in fabrication of printed electronic boards, flat antennas, or RFID cards with fast and easy production at low cost. Moreover, this technique shows a potential to print electrically conductive lines not only on flat surfaces but also on 3D objects. Recently, Ag nanoparticles have been used for fabrication of conductive inks for ink-jet printing. Ag nanoparticles have many advantages because the electrical conductivity of Ag is the best among metals, and it is also difficult to be oxidized under normal conditions [9, 10]. In this paper, we report a method to synthesize Ag nanoflakes with high concentration and suitable particle size for use as conductive material in conductive inks for ink-jet printing using electrohydrodynamic printing technique to print microelectronic boards. Electrical conductivity of inks depends on functional nanoparticles in the inks (Ag nanoparticles). We think that electrical conductivity of printed lines can be improved by increasing contact area of Ag nanoparticles in the lines. The Ag nanoflakes will have greater contact area than spherical particles, thus electrical conductivity of printed lines or microelectronic boards will be improved.

2. MATERIALS AND METHODS

2.1. Materials

Silver nitrate ($AgNO_3$) (Merck), trisodium citrate ($Na_3C_6H_5O_7$) (Merck), ascorbic acid ($C_6H_8O_6$) (Merck), sodium borohydride ($NaBH_4$) (Merck), cetyltrimethylammonium bromide ($C_{19}H_{42}NBr$) (Merck) were used as received.

2.2. Synthesis Method and Measurements

2.2.1. Synthesis method

Ag nanoparticles were synthesized by chemical reduction method using reducing agents to reduce Ag^+ ions to obtain metal nanoparticles. The mechanism of this synthesis is presented as followed:

$Ag^+ + X \rightarrow Ag^o \rightarrow$ nano Ag

In this mechanism, Ag^+ ions are first reduced by reducing agent X to form Ag^o atoms. After that, these atoms combine to form Ag nanoparticles. In this research, the synthesis of Ag nanoflakes included two steps. The first step was to synthesize Ag seed particles. $AgNO_3$ and $Na_3C_6H_5O$ were dissolved in DI water with concentrations of 0.05 M and 0.25 mM, respectively, followed by stirring for 10 minutes. After that, $NaBH_4$ solution (0.02 M) was added and the solution was stirred for 15 minutes to obtain the Ag seed particle solution (solution A). The second

step was the growing step of Ag seed particles to form Ag nanoflakes. $AgNO_3$ and CTAB were dissolved in DI water with concentrations of 0.05 M and 0.1 M, respectively, followed by adding $C_6H_8O_6$ solution (0.1 M) and stirred for 30 minutes to obtain solution B. After that, solution A was added into solution B and stirred for 30 minutes, followed by adding NaOH solution (5 M) dropwise to adjust pH.

2.2.2. Measurements

The obtained nanoparticles were characterized using X-ray diffractometer (XRD), ultraviolet-visible spectrometer (UV-Vis) (Cary 100), transmission electron microscope (TEM) (JEM model 1400, 100 kV). Particle size distribution was obtained using ImageJ software.

3. RESULTS AND DISCUSSION

3.1 The formation of Ag seed particles

In this research, Ag nanoflakes were synthesized by chemical reduction method using cetyltrimethylammonium bromide (CTAB) as a surfactant. The synthesis included two steps. The first step was to synthesize Ag seed particles. The seed particles were spherical Ag nanoparticles with small particle size in the range of 4 to 6 nm (Figure 2). The Ag seed particles were synthesized by chemical reduction method using trisodium citrate (TSC) as a surfactant and sodium borohydride as a reducing agent. The second step was the growing step of the Ag seed particles to form the Ag nanoflakes. In this step, ascorbic acid was used as a reducing agent to reduce Ag^+ ions with CTAB as a surfactant. The mechanism for the formation of the Ag nanoflakes is presented in Figure 1.

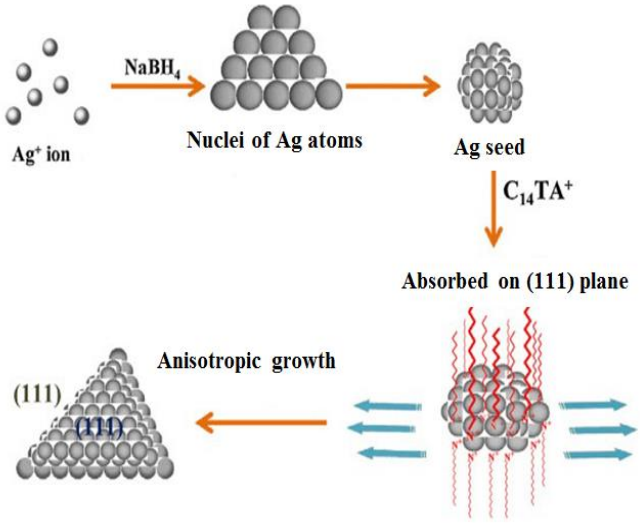

Figure 1. Mechanism for the formation of Ag nanoflakes using CTAB as surfactant

Because the adsorption of the CTAB molecules on the (111) plane was better than on the other planes, the CTAB molecules were adsorbed and covered this plane, inhibiting the growth of Ag particles in this direction. Thus, the Ag particles only grew in the directions parallel to the (111) plane to form the Ag nanoflakes.

Figure 2 shows the TEM image and particle size distribution of the Ag seed particles. The results show that the seed particles had spherical shape with particle size in the range of 4 - 6 nm.

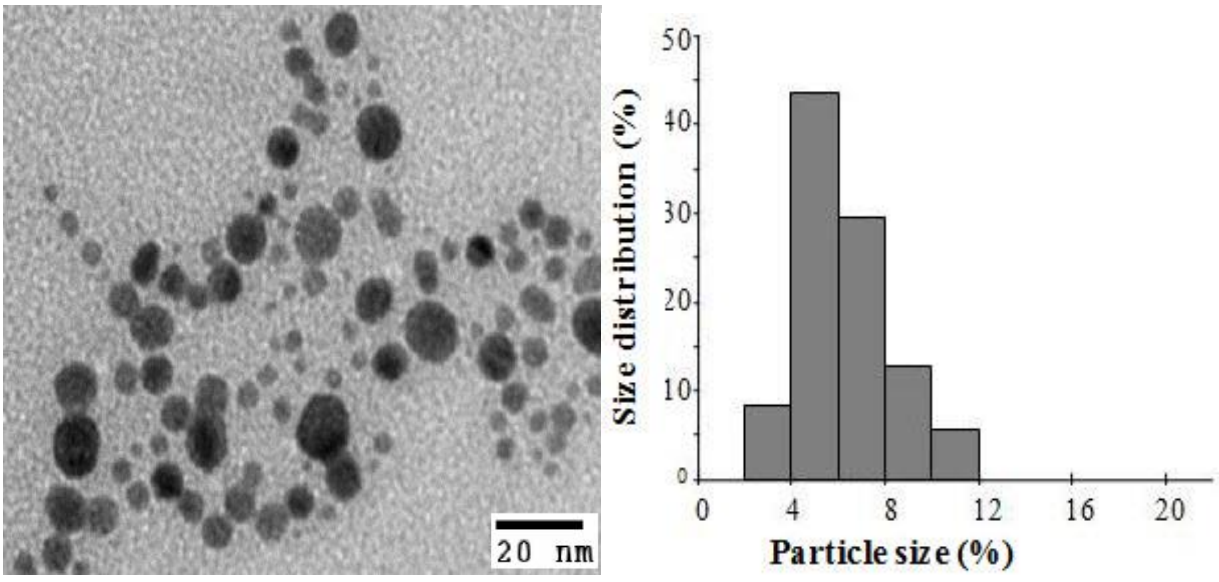

Figure 2. TEM image and particle size distribution of Ag seed particles

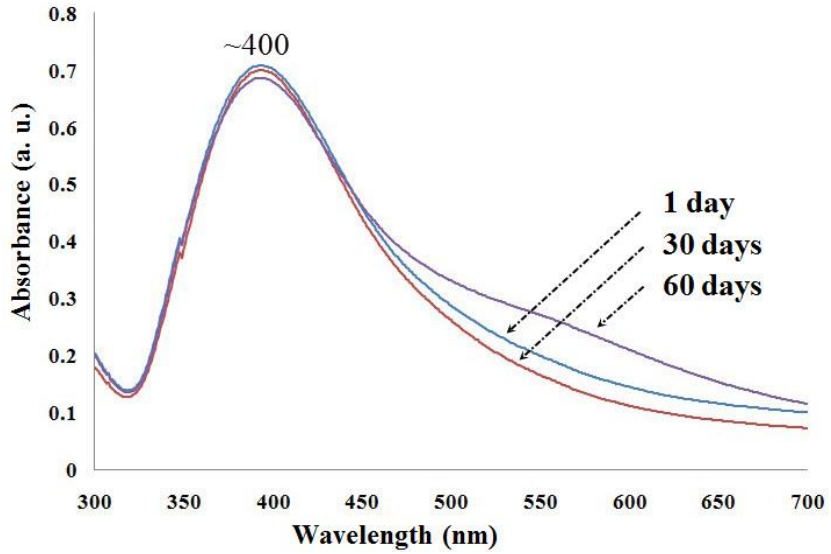

Figure 3. UV-Vis spectra of Ag seed particle solutions after different time from synthesis

Figure 3 shows the UV-Vis spectra of the Ag seed particle solutions after 1 day, 30 days, and 60 days from synthesis. The spectra of all samples exhibit an absorption peak at around 400 nm. The previous studies [11, 12] reported that Ag nanoparticles having spherical shape exhibited UV-Vis absorption peaks in the range of 390 - 450 nm depending on the uniformity and size of the particles (Mie theory). Thus, the results indicate the presence of Ag nanoparticles in the samples. Absorption intensity of the sample after 1 day was highest. After 30 and 60 days, the absorption intensity of the samples was reduced but not much. This indicated that the Ag seed particle solution was stable for a long time.

3.2. Effects of pH on the formation of the Ag nanoflakes

Metal nanoparticles dispersed in a solution always have a surface electric charge to avoid aggregation. The mechanism for the formation of electric charge depends on the properties of the metal nanoparticles and the solvent. In this method, we used DI water as solvent, thus the surface electric charge of the metal nanoparticles will be affected by the pH of the solution (Nernst equation). The samples were synthesized with different pH: 2, 4, 6, 8, 10, 12 to investigate the effects of pH on the formation of the Ag nanoflakes.

UV-Vis spectroscopy is an important analysis method with high accuracy in research of metal nanoparticles. This method is based on Mie theory and Lambert-Beer's law [13]. However, a limitation of the Mie theory is that it does not consider the optical resonance when metal nanoparticles are not spherical. The recent researches on Ag nanoflakes dispersed in solution reported that the UV-Vis spectra of the samples exhibited three absorption peaks, the first peak at around 325 - 350 nm, the second peak at around 400 - 450 nm, and the third peak at the longest wavelength [12, 14, 15]. These peaks were attributed to outer quadrupole resonance, outer dipole resonance, and inner dipole resonance, respectively [11, 12, 14, 15]. However, some other researches proposed different reasons for the appearance of the first and second peaks [16, 17].

Figure 4 shows that, the spectra of all the samples exhibit two peaks at around 425 nm and 530 - 550 nm. The spectra of the samples synthesized with pH=2 and pH=4 exhibit the third peak at around 345 nm with low intensity. The results indicate the presence of Ag nanoflakes in the samples. The peak at around 425 nm has higher intensity compared to that of the peak at around 530 - 550 nm. As presented above, the peak at around 425 nm was attributed to outer dipole resonance which was dominant for spherical Ag nanoparticles. Thus, the results suggest that the concentration of spherical Ag nanoparticles was higher than that of Ag nanoflakes in the samples.

The spectra of the samples synthesized with pH=2 and pH=4 exhibit the peak at around 345 nm. This peak was attributed to outer quadrupole resonance which gave information about thickness of Ag nanoflakes. Thus, these two samples had highest concentration of Ag nanoflakes.

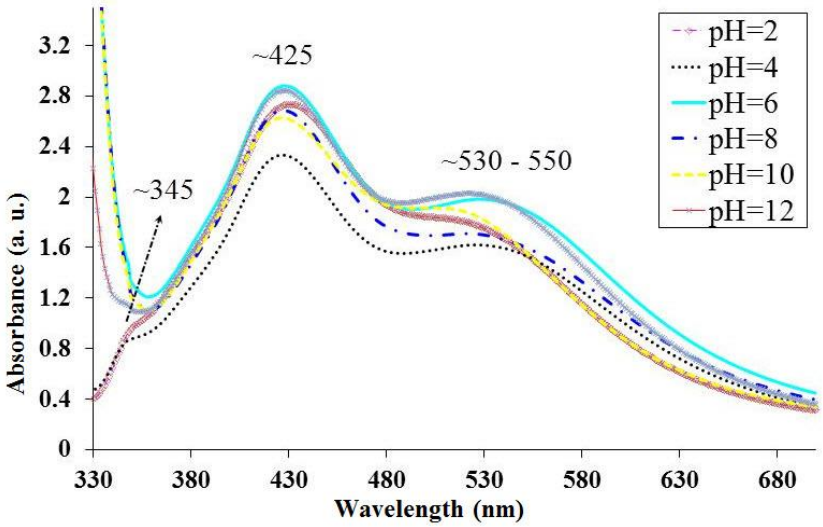

Figure 4. UV-Vis spectra of the samples synthesized with pH from 2 to 12

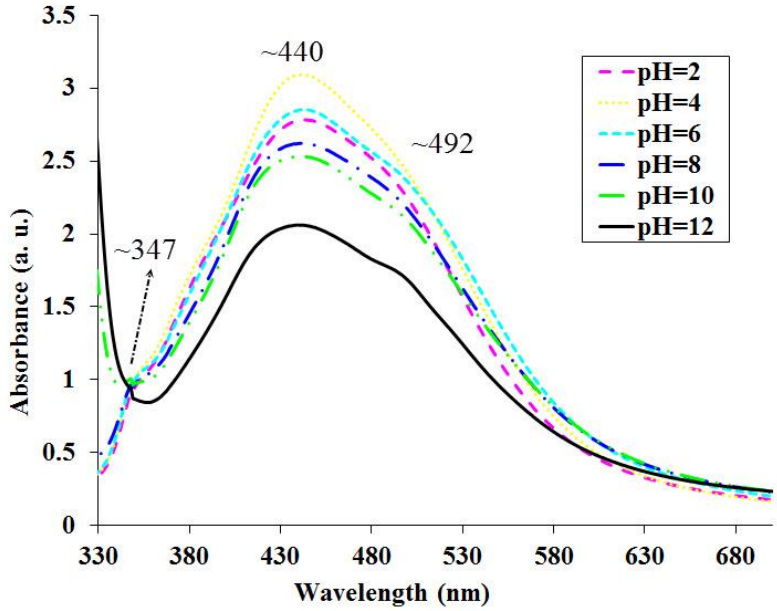

Figure 5. UV-Vis spectra of the samples after 60 days from synthesis

Figure 5 shows the UV-Vis spectra of the samples synthesized with different pH after 60 days from synthesis. The spectra show that, the second peak shifted to a longer wavelength at around 440 nm and the third peak shifted to a shorter wavelength at around 492 nm compared to the results of the samples measured just after synthesis. The second peak was also broader, suggesting the broader distributions of absorption centers and particle size. The third peak relates to the length of the Ag nanoflakes. This peak shifted to a shorter wavelength, suggesting the change of size and shape of the Ag nanoparticles. Figure 6 shows the change of intensity ratio of the second peak of the samples synthesized with pH = 2 and pH = 4 after 60 days from synthesis. The absorption intensity of the sample with pH = 2 was lower than that of the sample with pH = 4, indicating that the stability of the sample with pH = 4 was better. The spectrum of the sample with pH = 4 still exhibits three peaks of Ag nanoflakes, showing that this pH was optimal for this method.

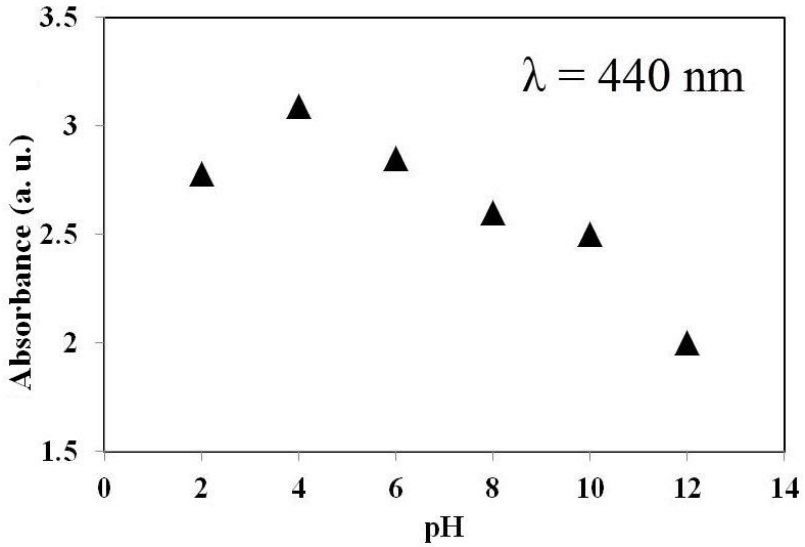

Figure 6. Absorption intensity at 440 nm of the samples synthesized with different pH after 60 days from synthesis

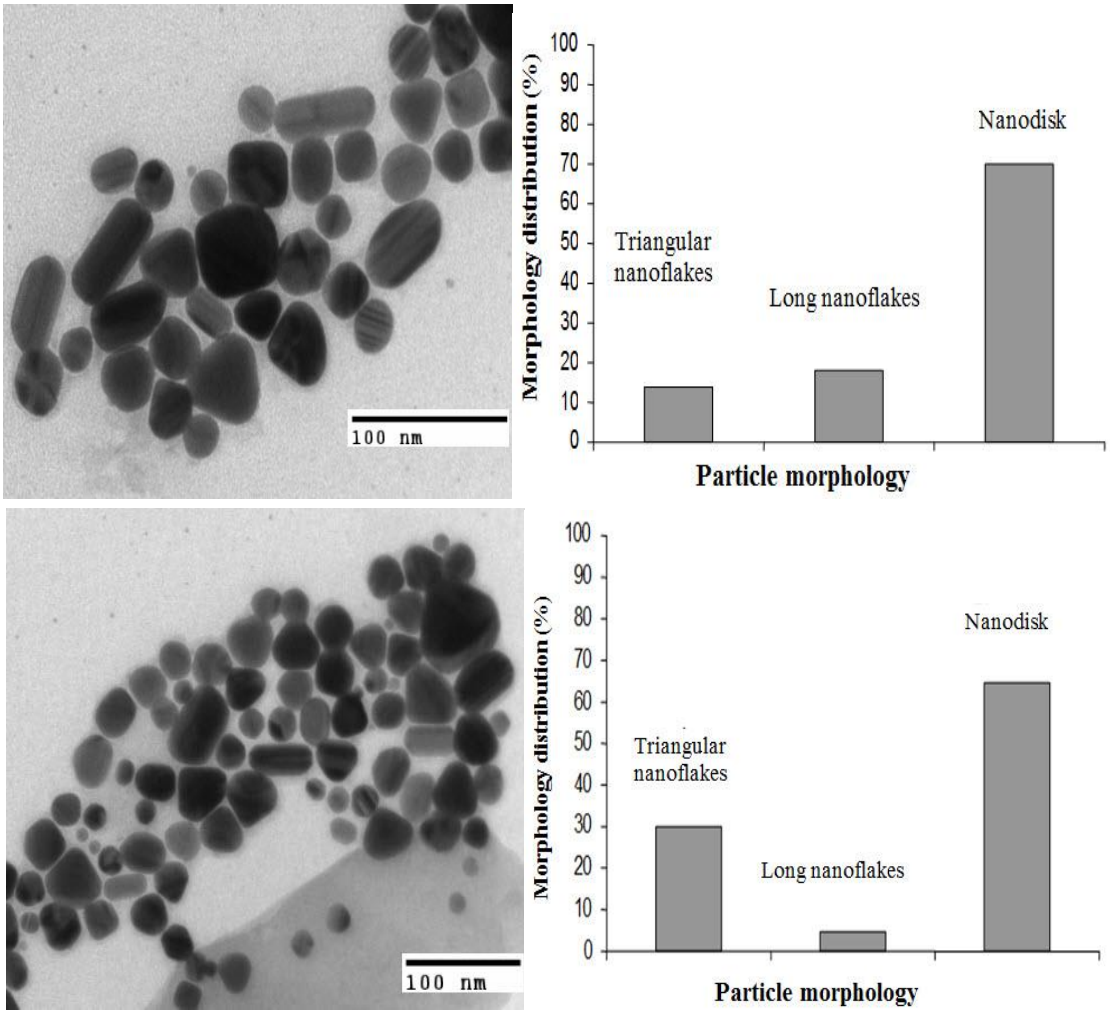

Figure 7. TEM images and shape distribution of Ag nanoparticles of the samples with pH=2 and pH=4

Figure 7 shows the formation of the Ag nanoparticles having different shapes including triangular nanoflakes, nanodisk, and long nanoflakes [10]. The Ag nanoparticles had a good dispersibility with average particle size of around 50-60 nm and thickness of the triangular nanoflakes of around 16 nm. Table 1 shows that content of Ag nanoflakes (including triangular nanoflakes and nanodisks) in the sample with pH=4 was 96 %, higher than that of the sample with pH=2 of 82 %.

Table 1. Shape distribution of Ag nanoparticles of the samples with pH=2 and pH=4

Samples	Ratio of triangular nanoflakes morphology (%)	Ratio of long nanoflakes morphology (%)	Ratio of nanodisk morphology (%)
pH=2	13	18	69
pH=4	30	4	66

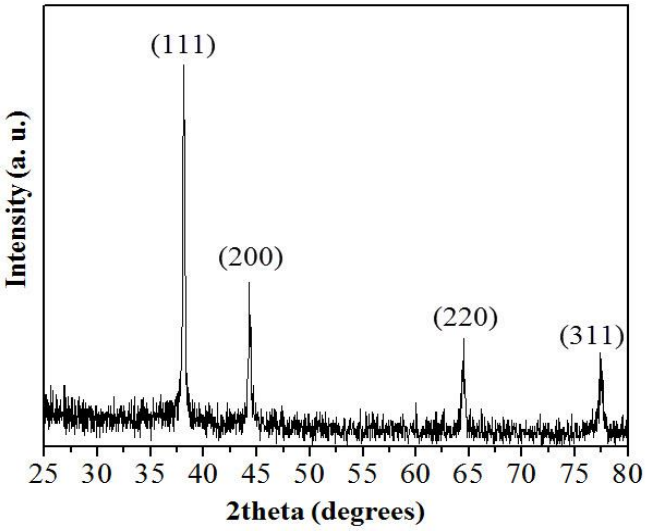

Figure 8. XRD pattern of the sample with pH=4.

To evaluate the crystallization and crystal structure of the Ag nanoflakes, XRD pattern of the sample with pH=4 was measured. Figure 8 shows the pattern of the sample, exhibiting the peaks at 36.19, 44.37, 64.56 and 76.47 degree, corresponding to the (111), (200), (220), (311) planes of cubic structure of Ag. The result shows that the Ag nanoflakes were well crystallized.

4. CONCLUSION

The Ag nanoflakes were synthesized by chemical reduction method using CTAB as a surfactant. The XRD, TEM, and UV-Vis results show that the obtained Ag nanoflakes had particle size of around 50 – 60 nm, thickness of around 16 nm, and content of the nanoflakes in the sample reached up to 96 %. The Ag nanoflakes crystallized in cubic structure of Ag. The Ag nanoflakes synthesized with pH = 4 dispersed stably after 60 days from synthesis under normal conditions. The properties of the obtained Ag nanoparticles were suitable for using them as conductive material in functional inks for ink-jet printing using electrohydrodynamic printing technique to print microelectronic boards.

Acknowledgements

The authors highly appreciate the financial support of FIRST Central Project Management Unit Grant Agreement. This research is funded by FIRST Central Project Management Unit Grant Agreement No.: 09/FIRST/2a/INT

REFERENCES

1. M.S. Bidoki, M.D. Lewis, M. Clark. Ink-jet fabrication of electronic components, Journal of Micromechanics and Microengineering, 17, 967–974, 2007.
2. K.B. Park, D. Kim, S. Jeong. Direct writing of copper conductive patterns by ink-jet printing, Thin Solid Films, 515, 7706–7711, 2007.
3. A. Apilux, Y. Ukita, M. Chikae, O. Chailapakul. Takamura, Y. Development of automated paper-based devices for sequential multistep sandwich enzyme-linked immunosorbent assays using inkjet printing. Lab Chip 13, 126–135, 2013.
4. M.C Dang, T.M.D. Dang, E. Fribourg-Blanc. Inkjet printing technology and conductive inks synthesis for microfabrication techniques. Adv. Nat. Sci.: Nanosci. Nanotechnol, 4, 15009–15016, 2013.
5. M.J. Meruga, M.W. Cross, S.P. May, A.Q. Luu, A.G. Crawford, J.J. Kellar. Security printing of covert quick response codes using upconverting nanoparticle inks. Nanotechnology, 23, 395201–39521, 2012.
6. K.B. Gupta, D. Haranath, S. Saini, N.V. Singh, V. Shanker. Synthesis and characterization of ultra-fine Y_2O_3: Eu^{3}+ nanophosphors for luminescent security ink applications. Nanotechnology, 21, 055607–055615, 2010.
7. C. D. Trinh, D. M. T. Dang, T. N. T. Le, T. T. Le, C. M. Dang. Synthesis and stability control of silver

nanoparticles prepared by using glucose as capping agent in chemical reduction method, Proceedings of IWNA (2013), Vung Tau, Vietnam 4, 608-613, 2013.

8. C.-L. Lee, K.-C.Chang, C.-M. Syu. Silver nanoplates as inkjet ink particles for metallization at a low baking temperature of 100oC, Physicochem. Eng 381, 85-91, 2011.
9. S. K. Volkman, Y. Pei, D. Redinger, S. Yin, V. Subramanian. Ink-jetted Silver/Copper conductors for printed RFID applications, Mat. Res. Soc. Symp. Proc 814, 1781-1786, 2004.
10. J. Liu, X. Li, X. Zeng. Silver nanoparticles prepared by chemical reduction-protection method, and their application in electrically conductive silver nanopaste, Journal of Alloys and Compounds 494, 84–87, 2010.
11. John michael Abendroth the photo-mediated synthesis of silver nanoprisms and tuning of their plasmonic properties, 2011.
12. Q. Lu, K.-J. Lee, K.-B.Lee, H.-T. Kim, J.Lee, N.V. Myung, Y.-H.Choa. Investigation of shape controlled silver nanoplates by a solvothermal process Journal of Colloid and Interface Science 342, 8–17, 2010.
13. J. R. Jiménez, F. Rodríguez-Marín, R. G. Anera, L. J. del Barco. Deviations of Lambert-Beer's law affect corneal refractive parameters after refractive surgery Optical Society of America 14, 5411, 2006.
14. Guan Mingyun, Shang Tongming, He Xianghong, Sun Jianhua, Zhou Quanfa, Gu Peng Synthesis of Silver Nanoplates without Agitation and Surfactant Rare Metal Materials and Engineering 40, 2069-2071, 2011.
15. Z. Yi, X. Li, X. Xu, B. Luo, J. Luo, W. Wu, Y. Tang. Green Effective chemical route for the synthesis of silver nanoplates in tannic acid aqueous solution Colloids and Surfaces A: Physicochem. Eng Aspects 392,131– 136, 2011.
16. T. Darmanin, P. Nativo, D. Gilliland, G. Ceccone, B. De Berardis, F. Guittard, F. Rossi, C. Pascual. Microwave-assisted synthesis of silver nanoprisms/nanoplates using a "modified polyolprocess" Colloids and Surfaces A: Physicochem.Eng 395,145–15, 2012.
17. Chien-Liang Lee, Ciou-Mei Syu, Hsueh-Ping Chiou, Chih-Hao Chen, Hao-Lin Yang High-yield Size-controlled synthesis of silver nanoplates and their applications as methanol-tolerant electrocatalysts in oxygen reduction reaction, International journal of hydrogen energy 36,10502-10512, 2011.